DESIGN OF MEMS-BASED MICROWAVE AND MILLIMETERWAVE SWITCHES FOR HIGH POWER APPLICATIONS

B. Ducarouge[1], E. Perret[3], F. Flourens[1], H. Aubert[3], J.W. Tao[3], X. Chauffleur[4], J.P. Fradin[4], D. Dubuc[1,2], K. Grenier[1], P. Pons[1], R. Plana[1,2]

[1]LAAS—CNRS, [2]P. Sabatier University, 7. Avenue du Colonel Roche, 31077 Toulouse Cedex 4, France
[3]LEN7—ENSEEIHT, 2 rue Charles Camichel, BP 7122 - F 31071 Toulouse Cedex 7, France
[4]EPSILON Ingénierie, California, Voie 5, BP 653; 31319 Labège Cedex, France, http://www.epsilon.fr
E-mail : ducarouge@laas.fr

Abstract—**This paper presents the design methodology of a MEMS-Based RF Switches for millimeterwave applications. Both microwave, electromechanical and high power handling performances are allowed thanks to an original topology of MEMS associated to an appropriate design methodology.**

1. INTRODUCTION

The use of MEMS switches for high performances millimeter-wave receivers is getting more and more attractive. Indeed the numerous advantages of MEMS devices (low power consumption, low losses, high isolation and high linearity) answer to the continuous rise of system performances requirements and their operating frequencies. MEMS devices have then advantageously been used in many receiver building blocks such as switching, tunable capacitor, phase shifter and reconfigurable filter [1], [2].

On the other hand, the introduction of MEMS in millimeter-wave emitters is not so impressive because the power capability of such devices remains to be evaluated and optimized. We propose in this paper a topology of RF MEMS Switches which exhibits a high power capability thanks to an appropriate design methodology. Moreover, this structure also features high microwave performances (insertion loss and isolation).

The second section presents the topology of MEMS switches investigated to achieve simultaneously high power capabilities and high microwave performances. The technological process is then summarized. The third section presents the study of the first limiting factor for high power handling: the electromigration effect. An electromagnetic method is presented and used to propose an optimum design of high power RF-Switches. The fourth section deals with the second limiting factor which can occur: the thermal effect. The last section is dedicated to the discussion of the results and to the conclusion.

0-7803-7821-0/03/$17.00

2. RF SWITCHES TOPOLOGY

The proposed topology for the high power MEMS switch is presented in Fig. 1. It is composed of a capacitive shunt bridge realized on a CPW line with two specific issues: (1) the switch is isolated from the CPW line and (2) the attracting electrodes are located on the CPW ground planes.

The design of such non—uniform width structure consists in making independent the optimizations of electrostatic (the actuation voltage), mechanical (the stiffness) and electromagnetic (the equivalent capacitor) performances. Indeed, on the one hand, the widths We and Wm (see Fig. 1) respectively control the stiffness and the pull down voltage. On the other hand, the insertion loss and the isolation of the RF MEMS switch are fixed by the width Wμ [3].

The concept of an isolated bridge translates into two interests: (1) the possible design of capacitive serial switches and (2) the simplicity of the attracting electrodes formed by the CPW ground planes.

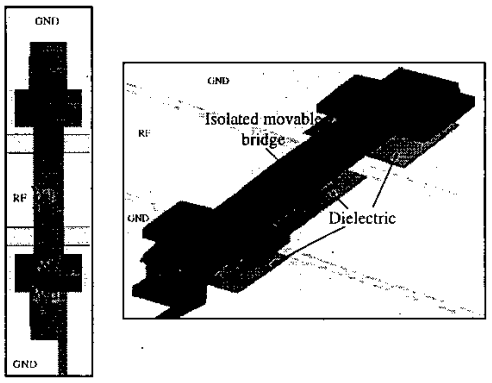

Fig. 1. Structure views.

This structure has been optimized using COVENTORWARE software and the results are: a pull down voltage of 30 V and a stiffness of 5 N/m.

In order to design and optimize more complex passive circuits, electrical models of switches are

necessary. In Fig. 2, we have defined a scalable equivalent electrical model from electromagnetic simulations (Sonnet) that allows a very fast optimization of the microwave performances.

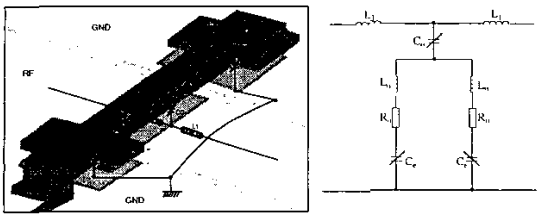

Fig. 2. Electrical model topology of the high power MEMS Switch.

The technological process of this structure uses surface micromachining to realize air-gap bridges [4].

First of all, a BCB layer is deposited on a HRS silicon substrate. Then are processed the gold coplanar line on top. An isolation dielectric layer between the line conductor and the bridge is patterned to avoid the stiction of the bridge when it is down.

The elaboration of the air-gap bridges begins with the patterning of a sacrificial photoresist to fix the anchorages. A thin seed metallic gold layer is evaporated on the photoresist and then gold is electroplated. After gold patterning, the sacrificial layer is etched by solvents.

3. E.M. DESIGN METHODOLOGY

This section presents the electromagnetic design methodology to evaluate the current density in the structure and warrants that the electromigration threshold or the maximum temperature are not achieved.

1. Approximation of the current density and the dissipated power density in a conductor-backed coplanar waveguide.

The Fig. 3 shows the cross-sectional view of the studied conductor-backed coplanar waveguide (CPWG). Because of its very low thickness (compared to the wavelength), the silicon oxide/nitride membrane is not taken into account in this simplified model. Moreover we consider a finite conductivity σ only for the CPWG discontinuity plane.

The characteristic impedance Z_C is known (Z_C is close to 70Ω for the dimensions given in Fig. 3).

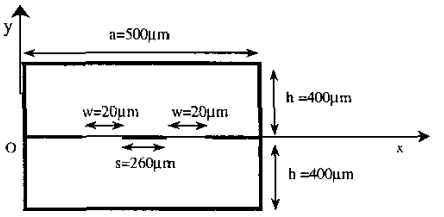

Fig. 3. Cross-sectional view of the studied CPWG.

The thickness t of the CPWG is large compared to the skin depth δ (in practice t = 3µm, and consequently, at 30GHz, the thickness is close to 10δ for CPWG manufactured in copper). Consequently, a surface impedance model can be advantageously used for taking into account the ohmic losses in the waveguiding structure. The dissipated power density in the CPWG is then approximated by $\frac{1}{2} Z_S J^2$ where J is the current density in the lossless case and, Z_S ($Z_S=1/\sigma\delta$) is the surface impedance.

The current density J is deduced from the Transverse Resonance Method. Since the width w of the slit is small compared to a, we adopt only one trial function for the representation of the electric field in the discontinuity plane. The current density J for y=0 is then given by the following analytical expression [5]:

$$J(x)=\frac{2\sqrt{2Z_C P_{EM}}}{Z_0\, a} \times \sum_{n=0,1,2,3,..} (-1)^n . \alpha_n \coth\left[(2n+1)\pi\frac{h}{a}\right] \sin\left[(2n+1)\frac{\pi}{2}\frac{s+w}{a}\right] J_0\left[(2n+1)\frac{\pi}{2}\frac{w}{a}\right] \sin\left[(2n+1)\frac{\pi}{a}x\right] \quad (1)$$

where P_{EM} is the electromagnetic power carrying by the TEM-mode along the CPWG (by assumption, the only one to propagate), Z_0 designates the free-space wave impedance ($Z_0=120\pi$) and J_0 represents the first kind and zeroth order Bessel function.

The current density J' for x = (a-s)/2 - w and $y \in [-t/2,0[$ is given by [5]:

$$J'(y)=\frac{2\sqrt{2\,Z_C\,P_{EM}}}{Z_0\, w}\left\{\sum_{n=1,2,3,..} (-1)^n\, J_0(n\pi)\, \frac{\mathrm{ch}\left[2n\frac{\pi}{w}\left(\frac{t}{2}+y\right)\right]}{\mathrm{ch}\left(n\pi\frac{t}{w}\right)}\right\} \quad (2)$$

where ch(x) designates the hyperbolic cosine of x.

For P_{EM} = 10W (carrying by the TEM-mode), the Fig. 4 and 5 display the dissipated power densities p_d and p'_d respectively. 2500 tones are used to compute p_d while 500 tones allows to reach the convergence for p'_d.

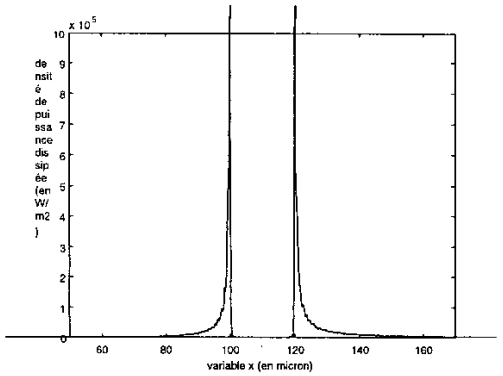

Fig. 4. dissipated power density p_d in the discontinuity plane of the CPWG shown in Fig. 3.

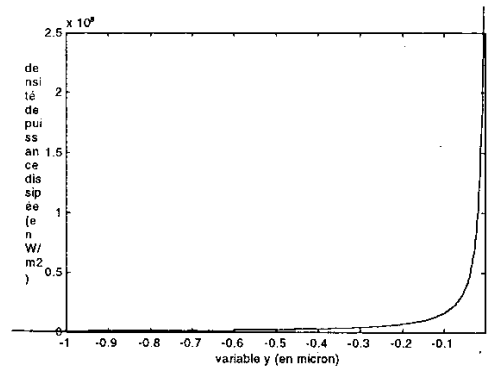

Fig. 5. Dissipated power density p'_d in the slit of the CPWG shown in Fig. 3.

From the current density, the electromigration phenomenon can be minimize through the suitable design of the line (see the following section) as from the dissipated power density, the temperature profile can be determined (see § 4).

2. Design methodology

Electromigration occurs under high current densities: atoms of conductive material are lifted by the current leading to open circuit failures. The critical current density above which electromigration effect happens is about J_{max}=1 MA / cm^2 in gold [6].

The previously presented method, associated with E.M. simulations (ANSOFT HFSS) in which the conductors have been meshed in volume, are used to estimate the maximum current density handled by 50 ohms coplanar and microstrip lines.

Maximum current densities of coplanar lines (made on a 20 µm thick BCB interlayer above silicon substrate) for different conductor and gap widths (resp. S and W) have been simulated. Microstrip lines on a 10 or 20 µm BCB layer (W: conductor width and t: BCB layer thickness) have also been evaluated. The maximum handling power depends on the specific incident power used for simulation: P_{SIMU}, the maximum current density simulated: J_{SIMU} and the electromigration threshold: J_{MAX}, according to:

$$P_{MAX}=P_{SIMU}\cdot\left(\frac{J_{MAX}}{J_{SIMU}}\right)^2 \qquad (3)$$

Table 1: Maximum power handled by CPW and microstrip lines.

Lines	microstrip		CPW		
Dimensions (µm)	S=25 t=10	S=50 t=20	S=90 W=10	S=180 W=50	S=250 W=100
Zc (Ohm)	50	50	52	50	48
Max power @ 10 GHz	**0.7 W**	**2.5 W**	**9 W**	**22 W**	**32 W**
Max power @ 20 GHz	**0.4 W**	**1.3 W**	**5 W**	**12 W**	**17 W**

The maximum powers for the different lines are reported in table 1. For this technology, wide coplanar lines are more suitable than microstrip ones for high power capabilities. Moreover, for a 30 W power handling application, coplanar line must exhibits a 250 µm central conductor width.

After this transmission line scaling, the following step addresses the design of a high power capabilities switch.

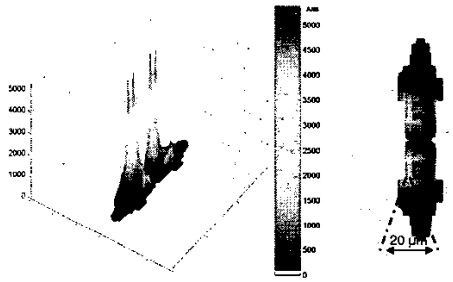

Fig. 6. Current density in power switch.

Figure 6 gives the simulated current density (using SONNET software) of the MEMS bridge realized on the previously investigated line (S= 250 W=100 µm) at down state for an incident power of 1 W at 20 GHz. It's worth noticing that the current density concentrates in the bridge edge (along 20 µm) on the CPW gaps. The maximum current density (5500 A/m) is close to the electromigration threshold at 20 GHz (5800 A/m) which limits the handling power to about 1.1 W. Further investigations on the bridge design are in progress to improve its power capability.

4. THERMAL MODELING

According to the results on power density, a thermal model of a CPW line has been performed using REBECA–3D software based on BEM and developed by EPSILON Ingénierie [7].

The CPW line is assumed to be realized on a two–layer membrane (2000x1300µm) as given in Fig. 7.

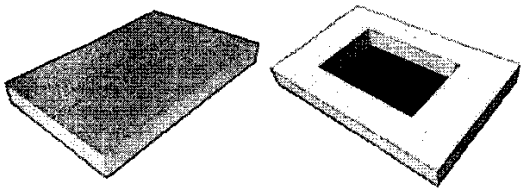

a) top side b) back side

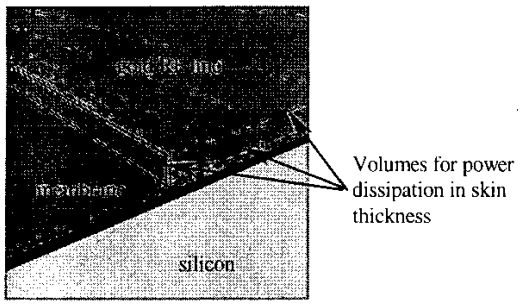

c) close view of a " coplanar gap "

Fig. 7. Thermal model

Power dissipation distribution along width of the RF device is redistributed as volumic power density in individual skin volume and power dissipation distribution along height of the "coplanar gap" is applied directly as flux power density (Fig.7c)).

Back side of silicon is assumed to be at uniform temperature of 25°C and only conductive heat exchange is considered (no convection).

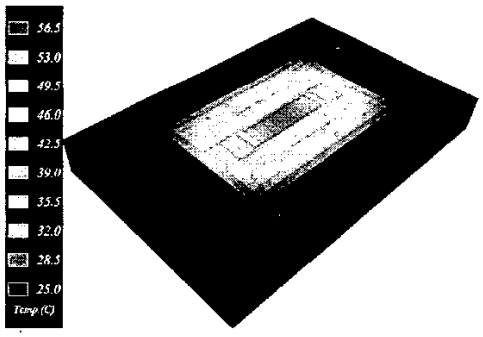

Fig. 8. Temperature distribution.

The Fig. 8 shows that the maximum temperature is located on the line and is of 56.5°C which means a rise of 31.5°C. Moreover, one notes that the part on the membrane is definitely hotter because of the strong thermal resistance of the latter.

Even if this rise is weak, mechanical study will be undertaken to check if the thermo-mechanical stresses are not sufficient to cause the buckling of the membrane in spite of its pre-tensioning.

These thermal studies outline that the temperature rise of the coplanar line doesn't translate into thermal failures. Similar studies on MEMS bridges are under investigation.

5. CONCLUSION

A MEMS-Based switch associated to a new design methodology has been proposed in this paper. A topology suitable for power handling capabilities has been simulated and optimized with respect to both electromechanical and microwave performances. A method to approximate current and power densities has been proposed in order to choose the best transmission line topology that accommodates the power requirements. Thermal simulations have shown that no critical temperature was reached. Nevertheless, improvements have to be done concerning the design of MEMS switch to prevent electromigration effect and to validate the complete design methodology.

Acknowledgement. This work was supported by the Midi-Pyrenées Region project called MEMSCOM in collaboration with Alcatel Space Industries.

References

[1] L. Dussopt, G.M. Rebeiz "High–Q Millimeter-Wave MEMS Varactors : Extended Tuning Range and Discrete-Position Designs", *IEE–MTTS*, Seattle–USA, 2002.

[2] J. DeNatale, R. Mihailovich, J. Hacker, J. Studer, G.M. Rebeiz, T.G. Leng, "Compact Low-Loss MEMS Phase Shifters", WorkShop, *IEEE-MTT–S*, Seattle–USA, 2002.

[3] B. Ducarouge, D. Dubuc, L. Rabbia, P. Pons, K. Grenier, R. Plana, "Structures optimisées de commutateurs MEMS RF", XIIIth National Microwaves Days, **3B** (2), May, Lille–France. 2003.

[4] K.Grenier, P. Pons, R. Plana, J. Graffeuil "Bulk Silicon Micro-machined MEMS Switches for Millimeter-Wave Applications" European Microwave Conference, London, United Kingdom, Sept., pp. 24–28, 2001.

[5] Hervé Aubert, "Calcul de la densité de puissance électromagnétique dissipée sur les parties métalliques d'une ligne coplanaire épaisse", in-house report, MEMSCOM Project, Mai 2003.

[6] J. B. Rizk, E. Chaiban, G.M. Rebeiz, "Steady State Thermal Analysis and High Power Reliability Considerations of RF MEMS Capacitive Switches", IEEE MTT-S Int. Microwave Symp. Dig., pp. 239–242, 2002.

[7] REBECA–3D : http://www.rebeca3d.com.